Proc. 8th German Microwave Conference (GeMiC)

A network model for evaluating MIMO backscatter systems considering mutual coupling

E. Denicke
B. Geck

A Network Model for Evaluating MIMO Backscatter Systems Considering Mutual Coupling

Eckhard Denicke, Bernd Geck
Institut für Hochfrequenztechnik und Funksysteme, Leibniz Universität Hannover
Appelstr. 9A, 30167 Hannover, Germany
Email: denicke@hft.uni-hannover.de, Tel.: +49 511 762-17227

***Abstract*—In this contribution a simulation framework for investigating arbitrary $M \times L \times N$ MIMO backscatter systems in terms of their communication capabilities is presented. The framework is implemented as a network model, based on various cascaded scattering parameter blocks representing the different parts of the dyadic communication link, i.e. the channel, the RFID reader transmit (TX) and receive (RX) antennas, the tag antennas as well as the TX/RX load impedances and the tag signaling matrix. The antenna mutual coupling at all three arrays is considered. With the model on the one hand e.g. the spatial multiplexing backscatter data transmission between tag and reader can be assessed in terms of the symbol error ratio. On the other hand theoretical figures of merit like the capacity of the transmission link can be investigated by determining the effective channel matrices for the forward and reverse link including the coupled antennas.**

***Index Terms*—multi-antenna RFID systems, MIMO, network model, mutual coupling, correlation, backscatter modulation, spatial multiplexing**

I. Introduction

Recenty, the application of multiple-input multiple-output (MIMO) techniques in backscatter-based radio-frequency identification (RFID) systems has seen continuously growing research attention. In contrast to ordinary MIMO communication links, multiple antennas can be applied at three locations in MIMO RFID systems, i.e. at the reader for transmitting (TX) and receiving (RX) and at the RFID tag as well ($M \times L \times N$ system [1]). Communication between tag and reader is done by scattering the reader continuous wave (CW) signal from the tag antennas back to the reader receive antennas in a modulated way through its signaling matrix (cp. [1]). The multiple antennas can be used for various purposes, e.g. for enhancing reliability, range or data rate.

It has been shown, that MIMO RFID systems can be adequately modeled with scattering parameters [2]. Thus, this contribution introduces a simulation framework for investigating arbitrary $M \times L \times N$ MIMO backscatter systems in terms of their communication capabilities.

In contrast to other publications, where only channel transmission coefficients are considered (e.g. [3]), the simulation framework accounts for the full scattering matrix between all antennas and can thus consider real world effects like e.g. antenna coupling at all three arrays.

Coupling effects in RFID systems have been e.g. investigated in the context of sensoring applications [4], RFID grids [5], passive tag-to-tag communication [6] or the read range of multiple tags [7]. To the knowledge of the authors the influence of mutual coupling especially at the tag on the communication properties of the system, e.g. on the spatial multiplexing efficiency, has not been investigated yet.

Thus, this paper will demonstrate the capabilities of the proposed simulation framework by assessing figures of merits like the theorical channel capacity or the symbol error ratio in dependence of the mutual coupling intensity.

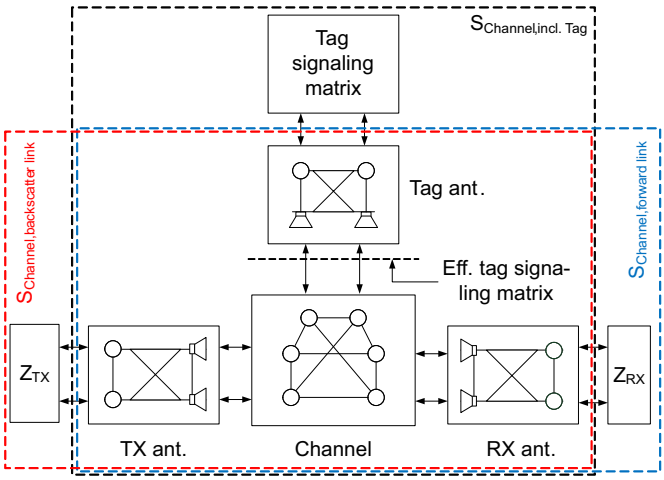

Figure 1. System model

II. Scattering Parameter based Network Model

Fig. 1 depicts the scheme of the network model, based on various scattering parameters blocks representing the different parts of the dyadic communication link, i.e. the channel, the M TX, N RX and L tag antennas as well as the tag signaling matrix. The scattering parameters matrices are connected in different ways using the mathematical descriptions for cascading scattering matrices or embedding them into each other (e.g. [8]). In contrast to similar network models proposed for usual MIMO systems (e.g. [9], [10]), in this case a third port group is introduced representing the RFID tag antennas.

Thus, on the one hand e.g. the data transmission on the forward link and, more interesting, the backscatter data transmission between tag and reader can be assessed e.g. in terms of the symbol error ratio. Therefore, the effective scattering matrix between the reader TX and RX ports is calculated in order to determine the signal transmission through the whole chain including the tag for all possible P^L modulation states of the signaling matrix (P-ary modulation scheme) (cp. $S_{\text{Channel,incl.Tag}}$ in Fig. 1). The received signal at the RX antennas for data modulation at the tag can then be easily

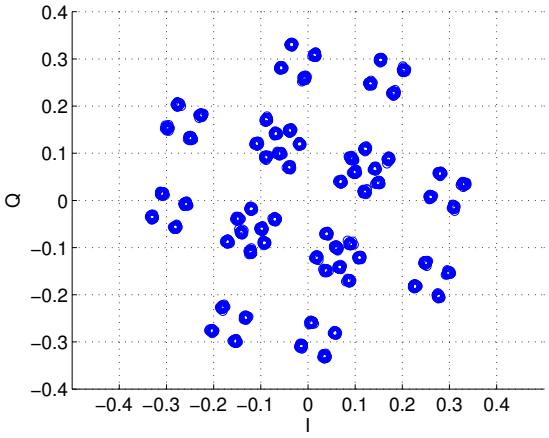

Figure 2. Exemplary $4^{L=3}$ constellation points, received at one RX-antenna

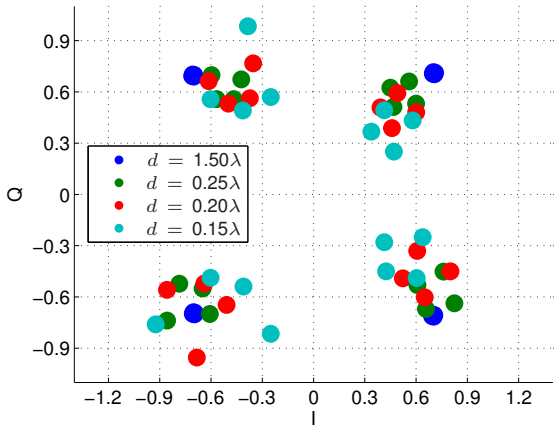

Figure 3. Effective constellation diagrams for various dipole distances d

simulated and evaluated (cp. Fig. 2 for an exemplary received constellation diagram within a $M \times 3 \times N$ system for one realization of rayleigh fading channel coefficients and QPSK backscatter modulation. The signal processing is adapted from our previous work [11].

On the other hand e.g. the capacity of the backscatter transmission link can be investigated by determining the effective forward ($S_{\text{Channel,forward link}}$) and backscatter/reverse link ($S_{\text{Channel,backscatter link}}$) scattering parameter matrices including the coupled antennas as input for the analytical theory (cp. [3]). The different scattering parameter blocks are described as follows.

A. Antennas

For all three arrays two thin wire dipole antennas of length $l \approx 0.48\lambda$, located side by side in a distance d, are assumed. Each array is considered as a scattering parameter block with two groups of ports, one for the antenna feed connection and one for the far field as well.

In this contribution the scattering matrices for the coupling as seen from the connection feeds have been obtained from the coupling impedance matrix for two equally oriented dipole antennas as implemented by [12], whereas the reference impedance is set - without loss of generality - to the (real) self impedance of each dipole.

For simplification, the transmission scattering parameter from the antenna feed to the farfield is assumed to be the square root of the radiated power (i.e. unity for lossless antennas, decreased by the power loss due to mismatch and power coupling into the other antenna). The structural reflection as seen from the farfield, which carries no backscatter information from the tag, but contributes to the static signal portion of the received signals, i.e. the carrier leakage, is neglected. For a more detailed modeling of the antennas, the generalized scattering matrix representation (e.g. [13]) could be implemented in future research. The correlation properties of the arrays in dependence of the mutual coupling are accounted for in the channel model (cp. Sec. II-B).

B. Channel

For the scattering matrix of the channel arbitrary models (accounting for the transmission between all antenna far field ports) can be implemented. In this contribution either ideal MIMO forward and backscatter channels (identity matrices) are assumed or the Kronecker stochastic channel model (cp. [14]) is employed to consider the correlation due to mutual coupling at all three arrays. For the latter case, the complex correlation coefficients at the TX, RX and tag array are obtained from the respective coupling scattering parameter formulation as seen from the feed connection (cp. [15]) (uniform distribution of the incoming and outgoing waves assumed), which are then used to create a multitude of rayleigh fading narrowband channel matrix realizations with corresponding correlation.

C. Signaling Matrix and TX/RX Terminations

Backscatter communication is done via switching the loads at the tag antenna ports, i.e. the reflection coefficients in the signaling matrix. Thus, this is modeled by terminating the tag antenna block with the tag signaling scattering matrix for all modulation states. Other terminations in the network model, which can be accounted for, are the mismatches of the reader TX or RX loads compared to the reference impedance.

III. Exemplary Simulation Results

A. Effective Tag Signaling Matrix incl. Tag Antenna Coupling

For backscatter spatial multiplexing the signaling matrix is a diagonal one, i.e. no transmission takes place in the load circuit between the tag antenna array feed ports. Nevertheless, when tag antenna coupling is introduced, a transmission between both antennas is present through the near field coupling. As shown in Fig. 1 the tag including coupling can be modeled as an effective tag signaling matrix $S_{\text{Signaling, eff.}}$, which can be calculated by embedding the original signaling matrix $S_{\text{Signaling}}$ into the tag coupling matrix S_{Tag}, i.e.:

$$S_{\text{Tag}} = \begin{bmatrix} S_{\text{Tag,FF,FF}} & S_{\text{Tag,FF,NF}} \\ S_{\text{Tag,NF,FF}} & S_{\text{Tag,NF,NF}} \end{bmatrix}, \tag{1}$$

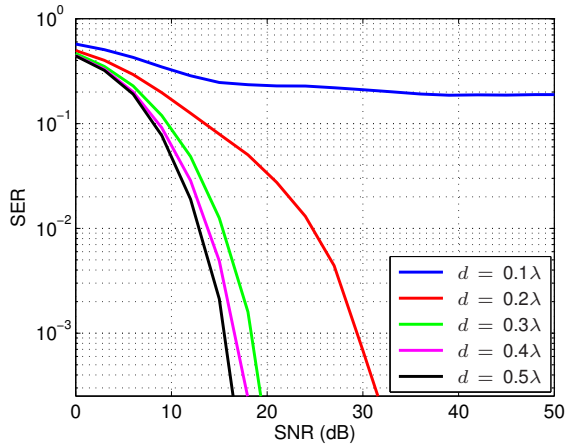

Figure 4. SER for different coupling intensities, i.e. dipole distances d

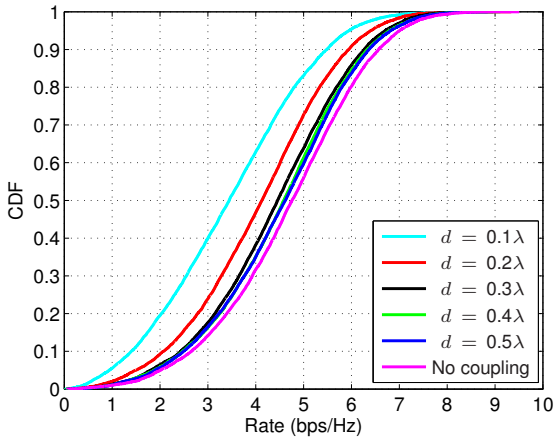

Figure 5. Cap. CDF ($2 \times 2 \times 2$) for diff. distances d (coupling only at tag)

$$S_{\text{Signaling, eff.}} = S_{\text{Tag,FF,FF}} + S_{\text{Tag,FF,NF}} \cdot \ldots \\ \ldots \cdot (S^{-1}_{\text{Signaling}} - S_{\text{Tag,NF,NF}})^{-1} \cdot S_{\text{Tag,NF,FF}} \ . \tag{2}$$

The port groups corresponding to the farfield and the feed connection are described by FF or NF, respectively.
Herein, a two dipole antenna tag with QPSK backscatter modulation is investigated, resulting in 4^2 modulation states of the signaling matrix. Thus, Fig. 3 shows the effective constellation diagrams seen from the far field at one tag antenna for various coupling intensities, i.e. dipole distances d Two effects can be observed: On the one hand, the antenna mismatch due to coupling introduces a deterioration of the constellation diagram from its original squared form (cp. $d = 1.50\lambda$), thus leading to a loss in modulation depth. On the other hand the near field coupling transmission between both antenna ports leads to some kind of double modulation, i.e. each constellation point is affected by an additional signal from the other antenna reflection coefficient, i.e. constellation point, and is thus split into another four points, resulting in 4^2 effective constellation points. Consequently, even in an ideal MIMO forward and backscatter channel (identity matrices) the individual modulation from each tag antenna load cannot be observed anymore independently from the other antenna's modulation.

B. Symbol Error Ratios for Spatial Multiplexing

Fig. 4 shows the symbol error ratios (SER) over signal-to-noise ratio (SNR) for backscatter spatial multiplexing in case of a $2 \times 2 \times 2$ system with uniform CW transmitter in an ideal forward and backscatter MIMO channel at various tag antenna distances d, i.e. mutual coupling intensities (minimum-mean-square-error (MMSE) receiver [16]). As expected the deteriorated constellation diagram for each antenna as described in Sec. III-A significantly impacts the demodulation and symbol decision. For too intense coupling, decision based on the original QPSK diagram is not possible, so other algorithms for adaptive constellation diagrams (cp. method 2 in [11]) could be used.

C. MIMO RFID Channel Capacity

In contrast to ordinary MIMO systems, the capacity of the backscatter link is individually effected by both the forward and the backscatter/reverse channel. The forward channel accounts for power delivery to the tag antennas for backscattering, whereas the backscatter channel has to rely on a rich scattering environment to achieve significant capacity. The capacity formulation for the forward link is identical to the one of ordinary MIMO systems, whereas the channel capacity formulation for the MIMO backscatter link is different and has been first proposed by [3]:

$$C = \log_2(\det[\mathrm{I} + \rho \mathrm{H}_b \mathrm{H}_f \mathrm{Q} \mathrm{H}_f^H \mathrm{H}_b^H]) \ , \\ \text{with } \mathrm{Q} = E[\mathrm{x}\mathrm{x}^H] \ . \tag{3}$$

Herein H_f and H_b are the forward and backscatter channel matrices, i.e. the respective transmission scattering parameter submatrices from $S_{\text{Channel,forward link}}$ and $S_{\text{Channel,backscatter link}}$. The SNR is denoted by ρ, x is the reader CW signal transmit vector, H is the conjugate transpose and E is the expectation. For simplification, herein Q is assumed for the uniform transmitter. Additionally Tr(Q) = 1 is considered. See e.g. [3] or [16] for information on designing the reader transmit signal properly to maximize performance. It should be noticed that the capacity formulation from [3] has to be extended in certain cases, since it does not include the influence of the tag signaling matrix. So, if e.g. the modulation states of the tag signaling matrix exhibit a reflectance of non-unity magnitude, the additional power loss has to be considered.
To investigate the effect of mutual coupling on the capacity in the following a $2 \times 2 \times 2$ backscatter system is assumed. The loads of TX and RX are matched to the reference impedance and there is no direct path from TX to RX in the channel (no carrier leakage).
The capacity was calculated at a mean SNR of $\rho = 10$ dB for 10000 channel realizations including different scenarios of coupling (and thus a deteriorated power flow and channel correlation).
Thus, in Fig. 5 the cumulative distribution function (CDF) of the backscatter link capacity is depicted for various dipole

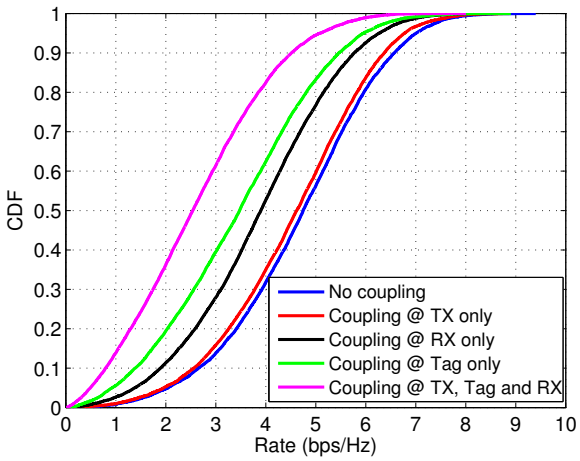

Figure 6. Cap. CDF ($2 \times 2 \times 2$) for different coupling situations ($d = 0.1\lambda$)

distances d, whereas coupling is assumed only at the tag. As expected, the capacity in general suffers from coupling, i.e. especially from small dipole distances.

Additionally, Fig. 6 shows the capacity CDF for different coupling situations, i.e. coupling is assumed at different arrays in the system (dipole spacing of $d = 0.1\lambda$). Obviously, coupling at all three array is the worst case, whereas coupling at the tag is worse in terms of the capacity than coupling at any other array. This is due to the fact, that the tag antennas are part of the forward and the backscatter channel as well, impacting both with power loss and correlation.

Moreover, it is interesting to notice, that the capacity for coupling at TX is higher than for coupling at RX, despite a comparable power loss for the whole transmission chain. This is due to the fact, that for the backscatter communication the forward channel only accounts for transmission of the CW signal, carrying no information. Thus, the forward channel correlation has less impact on the backscatter link capacity than the backscatter channel correlation.

IV. Conclusion

In this contribution a simulation framework for investigating arbitrary $M \times L \times N$ MIMO backscatter systems in terms of their communication capabilities is presented. In contrast to other publications the framework considers mutual coupling at all three antenna arrays in the system. It can be concluded that especially the tag antenna mutual coupling has different, more severe effects on the communication than the coupling in ordinary MIMO systems. The capabilities of the simulation framework have been shown by demonstrating e.g. the impact of coupling on the backscatter constellation diagram, the symbol error ratio or the capacity. Future work includes implementing more sophisticated channel and antenna models and investigating advanced signal processing schemes.

Acknowledgments

This work was supported by Deutsche Forschungsgemeinschaft, Grant GE 1667/3-1.

References

[1] J. Griffin and G. Durgin, "Gains for RF tags using multiple antennas," *Antennas and Propagation, IEEE Transactions on*, vol. 56, no. 2, pp. 563 –570, feb. 2008.

[2] E. Denicke, M. Henning, H. Rabe, and B. Geck, "The application of multiport theory for mimo rfid backscatter channel measurements," in *Microwave Conference (EuMC), 42nd European*, 2012, pp. 522 –525.

[3] M. Ingram, M. Demirkol, and D. Kim, "Transmit diversity and spatial multiplexing for rf links using modulated backscatter," in *Proceedings of the International Symposium on Signals, Systems, and Electronics, Tokyo, JAPAN*, July 24-27 2001.

[4] C. Paggi, C. Occhiuzzi, and G. Marrocco, "Sub-millimeter displacement sensing by passive uhf rfid antennas," *Antennas and Propagation, IEEE Transactions on*, vol. 62, no. 2, pp. 905–912, Feb 2014.

[5] G. Marrocco, "Rfid grids: Part i - electromagnetic theory," *Antennas and Propagation, IEEE Transactions on*, vol. 59, no. 3, pp. 1019 –1026, 2011.

[6] P. Nikitin, S. Ramamurthy, R. Martinez, and K. V. S. Rao, "Passive tag-to-tag communication," in *RFID (RFID), 2012 IEEE International Conference on*, April 2012, pp. 177–184.

[7] Y. Tanaka, Y. Umeda, O. Takyu, M. Nakayama, and K. Kodama, "Change of read range for uhf passive rfid tags in close proximity," in *RFID, 2009 IEEE International Conference on*, 2009, pp. 338 –345.

[8] J. A. Dobrowolski, *Microwave network design using the scattering matrix*. Norwood, MA, USA: Artech House, 2010.

[9] C. Waldschmidt, S. Schulteis, and W. Wiesbeck, "Complete rf system model for analysis of compact mimo arrays," *Vehicular Technology, IEEE Transactions on*, vol. 53, no. 3, pp. 579 – 586, May 2004.

[10] J. Wallace and M. Jensen, "Mutual coupling in mimo wireless systems: a rigorous network theory analysis," *Wireless Communications, IEEE Transactions on*, vol. 3, no. 4, pp. 1317 – 1325, 2004.

[11] E. Denicke, D. Härke, and B. Geck, "Investigating multi-antenna rfid systems by means of time-varying scattering parameters," in *Antennas and Propagation (EuCAP), 2013 7th European Conference on*, 2013, pp. 3314–3318.

[12] S. J. Orfanidis, *Electromagnetic Waves and Antennas*. Rutgers University, 2013. [Online]. Available: http://eceweb1.rutgers.edu/~orfanidi/ewa/

[13] Y. G. Kim and S. Nam, "Determination of the generalized scattering matrix of an antenna from characteristic modes," *Antennas and Propagation, IEEE Transactions on*, vol. 61, no. 9, pp. 4848–4852, Sept 2013.

[14] J. Kermoal, L. Schumacher, K. Pedersen, P. Mogensen, and F. Frederiksen, "A stochastic mimo radio channel model with experimental validation," *Selected Areas in Communications, IEEE Journal on*, vol. 20, no. 6, pp. 1211 – 1226, aug 2002.

[15] S. Blanch, J. Romeu, and I. Corbella, "Exact representation of antenna system diversity performance from input parameter description," *Electronics Letters*, vol. 39, no. 9, pp. 705–707, May 2003.

[16] F. Zheng and T. Kaiser, "On the transmit signal design at the reader for rfid mimo systems," in *RFID Technology (EURASIP RFID), 2012 Fourth International EURASIP Workshop on*, 2012, pp. 59–64.